



Retrospective Study

Computed tomography-based radiomics diagnostic approach for differential diagnosis between early- and late-stage pancreatic ductal adenocarcinoma

Shuai Ren, Li-Chao Qian, Ying-Ying Cao, Marcus J Daniels, Li-Na Song, Ying Tian, Zhong-Qiu Wang

Specialty type: Oncology

Provenance and peer review:

Invited article; Externally peer reviewed.

Peer-review model: Single blind

Peer-review report's scientific quality classification

Grade A (Excellent): 0

Grade B (Very good): 0

Grade C (Good): C, C

Grade D (Fair): 0

Grade E (Poor): 0

P-Reviewer: Zeng C, United States

Received: November 5, 2023

Peer-review started: November 5, 2023

First decision: December 20, 2023

Revised: December 27, 2023

Accepted: February 1, 2024

Article in press: February 1, 2024

Published online: April 15, 2024



Shuai Ren, Ying-Ying Cao, Li-Na Song, Ying Tian, Zhong-Qiu Wang, Department of Radiology, Jiangsu Province Hospital of Chinese Medicine, Affiliated Hospital of Nanjing University of Chinese Medicine, Nanjing 210029, Jiangsu Province, China

Li-Chao Qian, Department of Geratology, Nanjing Hospital of Chinese Medicine Affiliated to Nanjing University of Chinese Medicine, Nanjing 210022, Jiangsu Province, China

Marcus J Daniels, Department of Radiology, NYU Langone Health, New York, NY 10016, United States

Corresponding author: Zhong-Qiu Wang, MD, PhD, Deputy Director, Professor, Department of Radiology, Jiangsu Province Hospital of Chinese Medicine, Affiliated Hospital of Nanjing University of Chinese Medicine, No. 155 Hanzhong Road, Nanjing 210029, Jiangsu Province, China. zhongqiuwang0815@163.com

Abstract

BACKGROUND

One of the primary reasons for the dismal survival rates in pancreatic ductal adenocarcinoma (PDAC) is that most patients are usually diagnosed at late stages. There is an urgent unmet clinical need to identify and develop diagnostic methods that could precisely detect PDAC at its earliest stages.

AIM

To evaluate the potential value of radiomics analysis in the differentiation of early-stage PDAC from late-stage PDAC.

METHODS

A total of 71 patients with pathologically proved PDAC based on surgical resection who underwent contrast-enhanced computed tomography (CT) within 30 d prior to surgery were included in the study. Tumor staging was performed in accordance with the 8th edition of the American Joint Committee on Cancer staging system. Radiomics features were extracted from the region of interest (ROI) for each patient using Analysis Kit software. The most important and predictive radiomics features were selected using Mann-Whitney *U* test, univariate logistic regression analysis, and minimum redundancy maximum relevance (MRMR) method. Random forest (RF) method was used to construct the

radiomics model, and 10-times leave group out cross-validation (LGOCV) method was used to validate the robustness and reproducibility of the model.

RESULTS

A total of 792 radiomics features (396 from late arterial phase and 396 from portal venous phase) were extracted from the ROI for each patient using Analysis Kit software. Nine most important and predictive features were selected using Mann-Whitney *U* test, univariate logistic regression analysis, and MRMR method. RF method was used to construct the radiomics model with the nine most predictive radiomics features, which showed a high discriminative ability with 97.7% accuracy, 97.6% sensitivity, 97.8% specificity, 98.4% positive predictive value, and 96.8% negative predictive value. The radiomics model was proved to be robust and reproducible using 10-times LGOCV method with an average area under the curve of 0.75 by the average performance of the 10 newly built models.

CONCLUSION

The radiomics model based on CT could serve as a promising non-invasive method in differential diagnosis between early and late stage PDAC.

Key Words: Pancreatic ductal adenocarcinoma; Radiomics; Computed tomography; American Joint Committee on Cancer staging

©The Author(s) 2024. Published by Baishideng Publishing Group Inc. All rights reserved.

Core Tip: Pancreatic ductal adenocarcinoma (PDAC) remains the deadliest of the common cancers, with little change in patient survival in the past several decades. One of the biggest challenges of the management of PDAC that physicians often encounter is that the early detection in high-risk individuals and the early diagnosis of patients with suspected symptoms. Precise staging of PDAC is vital not only in making treatment decisions, but also in evaluating prognosis. Radiomics, the generation of minable high throughput data through conversion of digital computed tomography (CT) or magnetic resonance imaging, allows obtaining additional insight into pancreatic tissue heterogeneity. The aim of our study was to investigate a radiomics approach for potential differentiation of early- from late-stage PDAC. In conclusion, our study demonstrated that the radiomics model based on CT could serve as a promising non-invasive method in differential diagnosis between early and late stage PDAC. Large-scale prospective cohort studies, preferably multi-center, to validate the potential value of the radiomics diagnostic approach in differentiating early from late stage PDAC are in order.

Citation: Ren S, Qian LC, Cao YY, Daniels MJ, Song LN, Tian Y, Wang ZQ. Computed tomography-based radiomics diagnostic approach for differential diagnosis between early- and late-stage pancreatic ductal adenocarcinoma. *World J Gastrointest Oncol* 2024; 16(4): 1256-1267

URL: <https://www.wjgnet.com/1948-5204/full/v16/i4/1256.htm>

DOI: <https://dx.doi.org/10.4251/wjgo.v16.i4.1256>

INTRODUCTION

Pancreatic cancer remains one of the most dismal types of cancers worldwide, characterized by a poor prognosis and a low 5-year survival rate[1]. Pancreatic ductal adenocarcinoma (PDAC) constitutes more than 90% of all pancreatic cancer cases. PDAC is often diagnosed as advanced due to the anatomical structure of the deep retroperitoneal layer of the pancreas, lack of typical symptoms and effective screening methods[2]. PDAC is expected to surpass both breast and colorectal cancer as the second leading cause of cancer related deaths by year 2030[3].

One of the biggest challenges of the management of PDAC that physicians often encounter is that the early detection in high-risk individuals and the early diagnosis of patients with suspected symptoms. Two biomarkers including carbohydrate antigen 19-9 (CA 19-9) and carcinoembryonic antigen are recommended for screening PDAC in clinical practice[4,5]. CA 19-9 facilitates surgical decision and the detection of post-operative tumor recurrence; however, the utility of CA 19-9 is limited since 10% of patients do not secrete CA 19-9[6]. CA 19-9 levels are not found to be specific or sensitive enough for reliable detection of PDAC[5].

Multi-detector computed tomography (MDCT) is the most widely available and important pre-operative examination for patients with suspected PDAC[7]. MDCT provides good spatial resolution with wide anatomic coverage, which allows comprehensive evaluation of local and distant disease in a single session[8]. Notably, MDCT is proved to be a useful tool in assessment of vascular involvement, which is one of the deciding factors of tumor resectability[9,10]. The American Joint Committee on Cancer (AJCC) TNM staging criteria has been developed to characterize local and systemic spread PDAC. Precise staging of PDAC is vital not only in making treatment decisions, but also in evaluating prognoses [11]. The diagnosis and clinical staging of PDAC are established using CT and/or magnetic resonance imaging (MRI), or

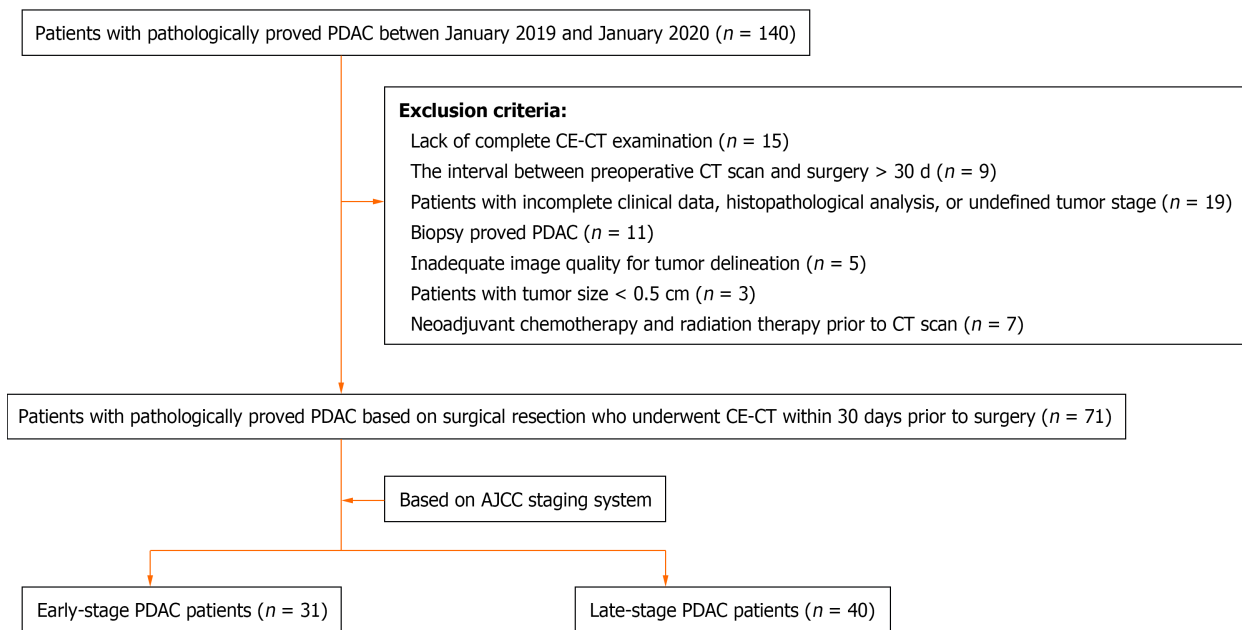


Figure 1 Flow diagram of patient inclusion. PDAC: Pancreatic ductal adenocarcinoma; CE-CT: Contrast-enhanced computed tomography; AJCC: American Joint Committee on Cancer.

endoscopic ultrasound-guided fine needle aspiration[12].

Over the past few years, radiomics has facilitated the development of processes for the conversion of digital images into mineable data and further analysis of the data for decision support. In clinical practice, the specific biopsy sample can provide histological information of tumors but may not reflect the full extent of the tumor phenotype due to sampling error[12]. Radiomics is a promising useful tool that assesses tissue gray-level intensity and pixel position in digital CT or MRI images and permits quantification of tumor spatial heterogeneity, which can preoperatively predict histological grade and guide clinical decision-making. Radiomics has been used for pathologic classification and TNM staging in different tumors and initial results are encouraging[13-15]. Recently, a well-written and insightful article by Xu *et al*[16] investigated the potential value of a circular RNA (circRNA)-based biomarker panel in distinguishing between early (stage I/II)- and late-stage (stage III/IV) PDAC, which appeared in the October 2023 issue of *Gastroenterology*. In our study, we also classified all PDAC into early (stage I/II)- and late-stage (stage III/IV), and investigated the potential value of radiomics model in distinguishing between early- and late- stage PDAC, which is critical for making strategic management decision and predicting prognoses.

MATERIALS AND METHODS

Patients

This study was approved by the ethics committee of Affiliated Hospital of Nanjing University of Chinese Medicine with waiver of informed consent due to its retrospective nature. The study was reviewed and approved by the ethics committee of Affiliated Hospital of Nanjing University of Chinese Medicine (Approval No. 2017NL-137-05). A total of 140 patients with pathologically proved PDAC from January 2019 to January 2020 was included in the study. Exclusion criteria were lack of complete contrast-enhanced CT examination (unenhanced, late arterial, and portal phases) ($n = 15$), the interval between preoperative CT scan and surgery > 30 d ($n = 9$), patients with incomplete clinical data, histopathological analysis, or undefined tumor stage ($n = 19$), biopsy proved PDAC ($n = 11$), inadequate image quality for tumor delineation ($n = 5$), patients with tumor size < 0.5 cm ($n = 3$), and neoadjuvant chemotherapy and radiation therapy prior to CT scan ($n = 7$). Finally, 71 patients with pathologically proved PDAC (39 males and 32 females with a mean age of 61.55 ± 8.53) were included in the study. Tumor staging was performed in accordance with the most current AJCC staging system (the 8th edition)[11]. A total of 71 patients were classified into stage IA ($n = 4$), stage IB ($n = 8$), stage IIA ($n = 3$), stage IIB ($n = 16$), stage III ($n = 16$) and stage IV ($n = 24$). Finally, patients with PDAC were defined as early-stage (I-II) and late stage (III-IV) (Figure 1).

CT examination

All patients underwent triple-phase CT scan including unenhanced, late arterial, and portal venous phases. CT scanning was completed using one of the following scanners: (1) GE Optima 670 (GE Healthcare, Tokyo, Japan); (2) GE Lightspeed 64 VCT (GE Healthcare); (3) SIMENS SOMATOM Definition; and (4) Philips Brilliance 64 (Philips Healthcare, DA Best, the Netherlands). The following scan parameters were used: Tube voltage, 120Kvp; tube current, 200-400 mAs; helical pitch, 0.984-1.375; and 1.0 mm reconstruction slice thickness with an interval of 1.0 mm. An administration of 100-120 mL

nonionic contrast media (Omnipaque 350, Bayer Pharmaceuticals) at a rate of 3.0-4.0 mL/s was performed after the unenhanced CT scan. The late arterial and portal venous phases were acquired at 35 s and 70 s, respectively.

Image analysis

The CT images were retrospectively reviewed by two abdominal radiologists in consensus. Any disparity was resolved by referring to a senior radiologist with 15 years' experience of reading abdominal CT images. The following CT imaging features were evaluated in consensus: Tumor location, tumor margin (well-defined or ill-defined margin), presence of calcification, presence of cystic degeneration, presence of pancreatic duct dilatation, presence of vascular invasion, presence of lymph node metastasis, and presence of distal metastasis. Well-defined margin represents a margin that is smooth and visible, while spiculation or infiltration on one quarter of tumor perimeter indicates an ill-defined margin [17]. Calcifications were identified on unenhanced CT images. Cystic degeneration within the tumor was defined as low attenuation areas with CT attenuation values < 20 Hounsfield units or lack of enhancement on contrast-enhanced CT [18]. A maximal diameter ≥ 3 mm indicates pancreatic duct dilatation. Vascular invasion was defined in accordance with National Comprehensive Cancer Network guideline (version 2.2019-April 9, 2019) [19].

Tumor segmentation

Dual-phase pancreatic CT protocol including late arterial and portal venous phases were recommended for the optimal evaluation of primary pancreatic tumors. In the present study, ITK-SNAP software (version 3.6.0) was used for tumor segmentation on the late arterial and portal venous phase images and regions of interest (ROIs) were manually outlined by the side of the complete tumor margin on all contiguous slices by an experienced radiologist, who was blinded to the histopathological and clinical findings of these patients and used ITK-SNAP for other studies consisting of 221 patients with confirmed pancreatic diseases [20,21].

Feature extraction and selection

Prior to feature extraction, gray-level normalization (a unified voxel size of 1.0 mm \times 1.0 mm \times 1.0 mm) was carried out in order to exclude disturbances caused by scanner variabilities and parameters before radiomics analysis [21]. A total of 792 radiomics features (396 from late arterial phase and 396 from portal venous phase) were extracted from the ROIs for each patient using Analysis Kit software (version V3.0.0.R, GE Healthcare). Mann-Whitney *U* test, univariate logistic regression analysis, and minimum redundancy maximum relevance (MRMR) method were used to identify the most pivotal and predictive radiomics features from all features in differential diagnosis between early-stage and late-stage PDAC.

Construction and validation of radiomics model

The selected features from the late arterial and portal venous phases were used to construct the radiomics model using random forest (RF) method, which grows multiple decision trees that are merged together for a more accurate prediction. The prediction ability of the radiomics model was assessed and recorded.

The robustness and reproducibility of the radiomics model was validated using 10-times leave group out cross-validation (LGOCV) method. Patients were randomly divided into training and validation sets at a ratio of 7:3 for 10 times. For each time, a radiomics model was generated in the training set and the validation set was used to evaluate the predictive ability of the radiomics model. The robustness and reproducibility of the radiomics model was shown by the average performance of the 10 newly built models.

Statistical analysis

Statistical analysis was performed using SPSS v.24 (IBM Corp., Chicago, LA, United States) and R software v.3.6.1. *P* < 0.05 was considered to be statistically significant.

RESULTS

Demographic characteristics

A total of 71 PDAC patients with a mean age of 61.55 ± 8.53 years were classified into early-stage (*n* = 31) and late-stage (*n* = 40) based on AJCC TNM staging criteria. The demographic characteristics were listed in Table 1. No statistically significant difference was found with respect to patients' age (61.45 ± 8.93 years *vs* 61.63 ± 8.31 years, *P* = 0.933), sex, or demographic characteristics.

CT findings

CT findings of patients with early-stage and late-stage PDAC were listed in Table 2. No statistically significant difference was found with respect to tumor location, tumor margin, calcification, cystic degeneration, pancreatic duct dilatation, vascular invasion, or lymph node metastasis. Late-stage PDAC has a larger tumor size as compared to early-stage PDAC (4.03 ± 1.25 cm *vs* 3.05 ± 0.54 cm, *P* < 0.001). Late-stage PDAC has a higher frequency of distal metastasis as compared to early-stage PDAC [24 (60%) *vs* 0 (0%), *P* < 0.001]. Two representative cases of early-stage and late-stage PDAC were shown in Figure 2. Case 1 represents a patient with stage IB PDAC, which located at the tail of the pancreas (Figure 2A-C). Case 2 represents a patient with stage IV PDAC, which located at the tail of the pancreas (Figure 2D-F).

Table 1 Demographic characteristics of patients with early-stage and late-stage pancreatic ductal adenocarcinoma

Characteristic	Clinical stage classification		P value
	Early-stage PDAC (n = 31)	Late-stage PDAC (n = 40)	
Age (yr)	61.45 ± 8.93	61.63 ± 8.31	0.933
Sex			0.153
Male	20 (64.5%)	19 (47.5%)	
Female	11 (35.5%)	21 (52.5%)	
Abdominal pain	14 (45.2%)	20 (50%)	0.686
Abdominal bloating	8 (25.8%)	11 (27.5%)	0.873
Abdominal discomfort	16 (51.6%)	21 (52.5%)	0.941
Body weight loss	11 (35.5%)	14 (35.0%)	0.966
Jaundice	7 (22.6%)	9 (22.5%)	0.994
AJCC staging			-
IA	4 (12.9%)		
IB	8 (25.8%)		
IIA	3 (9.7%)		
IIB	16 (51.6%)		
III	0	16 (40%)	
IV	0	24 (60%)	

PDAC: Pancreatic ductal adenocarcinoma; AJCC: American Joint Committee on Cancer.

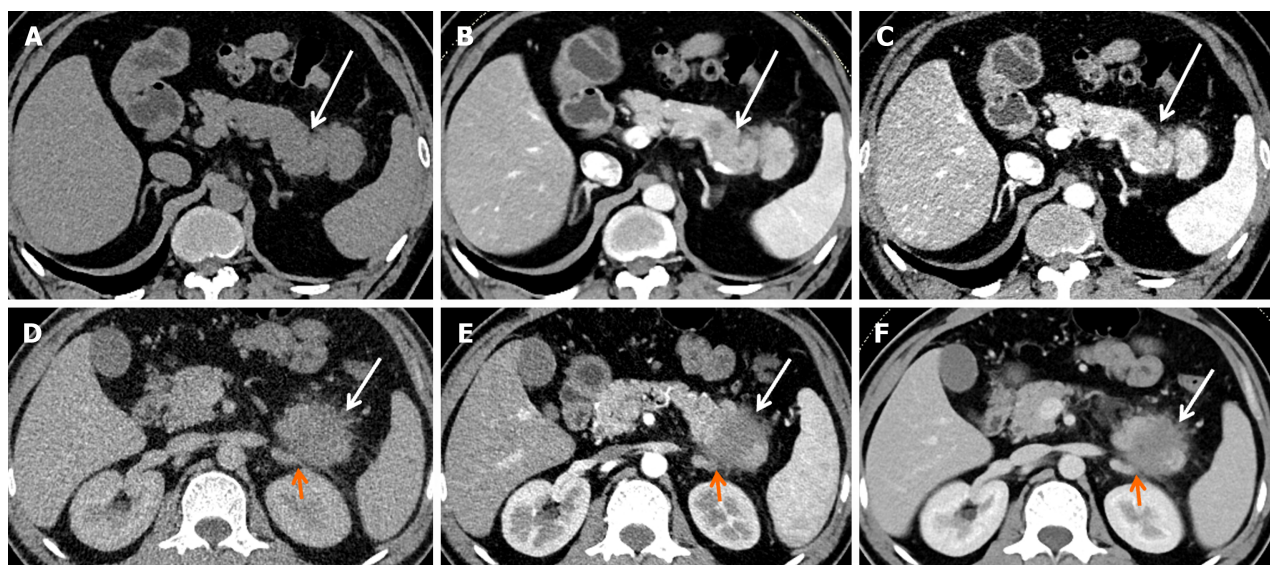


Figure 2 Computed tomography images of two representative cases of pancreatic ductal adenocarcinoma. A-C: A 54-year-old man with stage IB pancreatic ductal adenocarcinoma (PDAC). Computed tomography (CT) imaging showed a well-defined, predominantly solid tumor (white arrow), 3.0 cm in diameter in the tail of the pancreas. No obvious lymph node metastasis, vascular invasion, or distal metastasis was found. TNM classification: T2N0M0 (IB); D-F: A 44-year-old man with stage IV PDAC. CT imaging showed an ill-defined, predominantly solid tumor (white arrow), 4.1 cm in diameter in the tail of the pancreas. The left adrenal gland (orange arrow) was grossly invaded by the tumor. TNM classification: T3N1M1 (IV).

Feature extraction and selection

The extracted radiomics features from each phase CT imaging included histogram features ($n = 42$), morphological features ($n = 9$), grey level co-occurrence matrix (GLCM) features ($n = 144$), grey level size zone matrix features ($n = 11$), grey level run-length matrix features ($n = 180$), and Haralick features ($n = 10$).

Table 2 Computed tomography findings of patients with early-stage and late-stage pancreatic ductal adenocarcinoma

Characteristic	Clinical stage classification		P value
	Early-stage PDAC (n = 31)	Late-stage PDAC (n = 40)	
Tumor size (cm)	4.03 ± 1.25	3.05 ± 0.54	< 0.001
Tumor location			0.869
Head & neck	18 (58.1%)	24 (60.0%)	
Body & tail	13 (41.9%)	16 (40.0%)	
Tumor margin			0.722
Well-defined	4 (12.9%)	3 (7.5%)	
Ill-defined	27 (87.1%)	37 (92.5%)	
Calcification			1.0
Y	1 (3.2%)	1 (2.5%)	
N	30 (96.8%)	39 (97.5%)	
Cystic degeneration			0.757
Y	3 (9.7%)	6 (15.0%)	
N	28 (90.3%)	34 (85.0%)	
MPD			0.861
Y	20 (64.5)	25 (62.5%)	
N	11 (35.5)	15 (37.5%)	
Vascular invasion			0.302
Y	14 (45.2%)	23 (57.5%)	
N	17 (54.8%)	17 (42.5%)	
Lymph node metastasis			0.480
Y	16 (51.6%)	24 (60.0%)	
N	15 (48.4%)	16 (40.0%)	
Distal metastasis			< 0.001
Y	0 (0%)	24 (60%)	
N	31 (100%)	16 (40%)	

Categorical variables were presented as the number of cases (%) and were analyzed by using χ^2 or Fisher's exact tests. MPD: Main pancreatic duct dilatation; PDAC: Pancreatic ductal adenocarcinoma.

Nine most important and predictive radiomics features were identified after feature selection using Mann-Whitney *U* test, univariate logistic regression analysis, and MRMR method. Among them, 6 features were extracted from the late arterial phase (named a _ feature) and the others from the portal venous phase (named p _ feature). The selected features were a_Correlation_angle135_offset4, p_Correlation_angle90_offset7, a_Correlation_angle45_offset7, a_GLCM-Entropy_AllDirection_offset4_SD, a_Compactness2, a_GLCMEntropy_AllDirection_offset7_SD, p_Compactness2, a_InverseDifferenceMoment_AllDirection_offset4_SD, and p_HighGreyLevelRunEmphasis_AllDirection_offset. The histograms of cases 1 and 2 were shown in Figure 3, which demonstrated a marked difference. The area under the receiver operating characteristic curve (AUC) barplot of the selected radiomics features were shown in Figure 4A. The importance of the selected radiomics features were shown in Figure 4B. Figure 4C is a heatmap showing expression values of the selected radiomics features (rows) of 71 PDAC patients (columns). The differential diagnostic ability of the selected radiomics features were listed in Table 3, including AUC value, sensitivity, specificity, and accuracy.

Construction and validation of radiomics model

We subsequently adopted RF method to construct a radiomics model to differentiate between early-stage and late-stage PDAC, which had an AUC of 0.99 (Figure 5A). The RF classifier showed a high discriminative ability with 97.7% accuracy, 97.6% sensitivity, 97.8% specificity, 98.4% positive predictive value, and 96.8% negative predictive value. We finally used 10-times LGOCV method to validate the robustness and reproducibility of the radiomics model, with a mean AUC of 0.75 by the average performance of the 10 newly built models (Figure 5B), indicating good predictive ability of

Table 3 The differential diagnostic ability of the selected radiomics features

Features	AUC	SEN	SPE	ACC
a_Compactness2	0.754	67.5%	77.42%	71.83%
a_GLCMEntropy_AllDirection_offset7_SD	0.698	82.5%	58.06%	71.83%
p_Correlation_angle90_offset7	0.683	60.0%	70.97%	64.79%
p_HighGreyLevelRunEmphasis_AllDirection_offset4_SD	0.661	77.5%	51.61%	66.20%
a_GLCMEntropy_AllDirection_offset4_SD	0.665	87.5%	54.84%	73.24%
a_Correlation_angle45_offset7	0.639	50.0%	77.42%	61.97%
p_Compactness2	0.66	80.0%	54.84%	69.01%
a_InverseDifferenceMoment_AllDirection_offset4_SD	0.638	75.0%	64.52%	70.42%
a_Correlation_angle135_offset4	0.677	75.0%	58.06%	67.61%

AUC: Area under the receiver operating characteristic curve; SEN: Sensitivity; SPE: Specificity; ACC: Accuracy; GLCM: Grey level co-occurrence matrix.

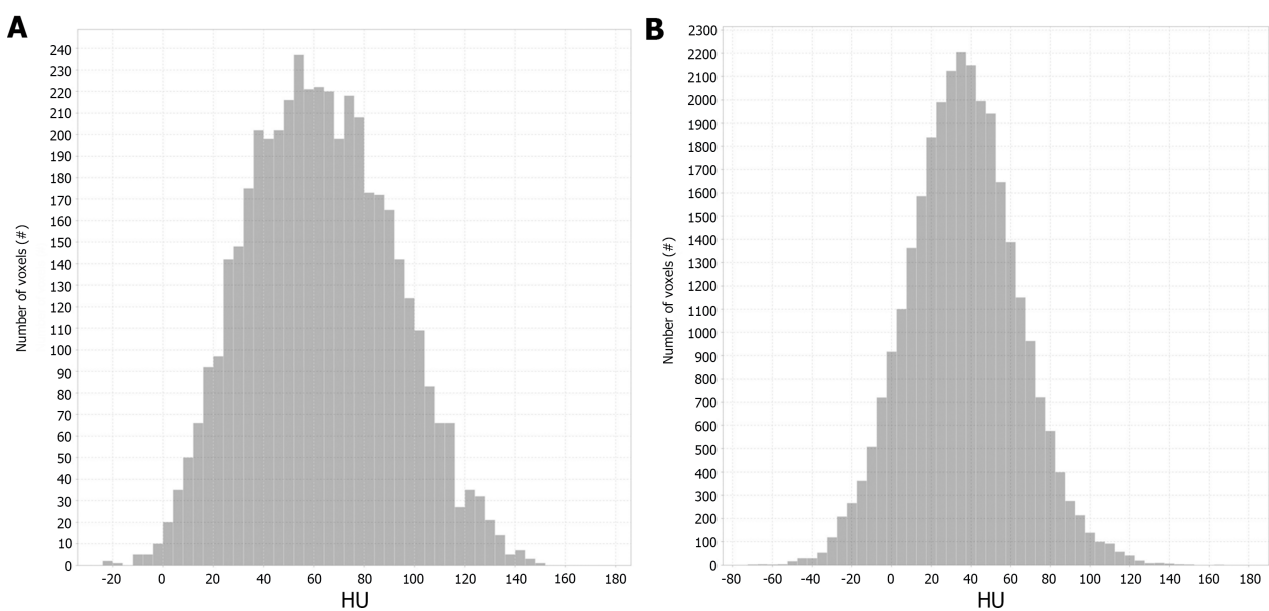


Figure 3 Histograms of two representative cases of pancreatic ductal adenocarcinoma. A and B: Stage IB pancreatic ductal adenocarcinoma (PDAC), A vs stage IV PDAC, B, which showed a marked difference. The X-axis indicates the gray level (HU). The Y-axis indicates the number of voxels.

the radiomics model.

DISCUSSION

In the present study, we developed and validated a radiomics model in differentiating early-stage PDAC from late-stage PDAC. The radiomics model incorporating the most important and predictive features selected using Mann-Whitney *U* test, univariate logistic regression analysis, and MRMR method, displayed a high discriminative ability. The results demonstrated that radiomics analysis may facilitate the preoperative risk stratification, clinical decision making, and maximize patient survival in patients with PDAC with short life expectancy.

The accurate staging of PDAC and assessment of surgical resectability is crucial in the management of this dismal disease[22]. Xu *et al*[16] classified PDAC into early (stage I/II)- and late-stage (stage III/IV) and evaluated the diagnostic ability of a circRNA-based biomarker panel in distinguishing between them. In our study, patients with PDAC were also grouped as early-stage (I-II) and late stage (III-IV). No statistically significant difference was found with respect to patients' age, sex, or demographic characteristics between early-stage and late-stage PDAC. This implied that early-stage and late-stage PDAC could not be differentiated by the demographic characteristics. The importance of tumor size was further underlined in the latest version of AJCC, especially for further grouping of T1-stage PDAC[22]. After CT imaging interpretation, late-stage PDAC has a larger tumor size as compared to early-stage PDAC (4.03 ± 1.25 cm *vs* 3.05 ± 0.54 cm, *P* < 0.001). Additionally, late-stage PDAC has a higher frequency of distal metastasis as compared to early-stage

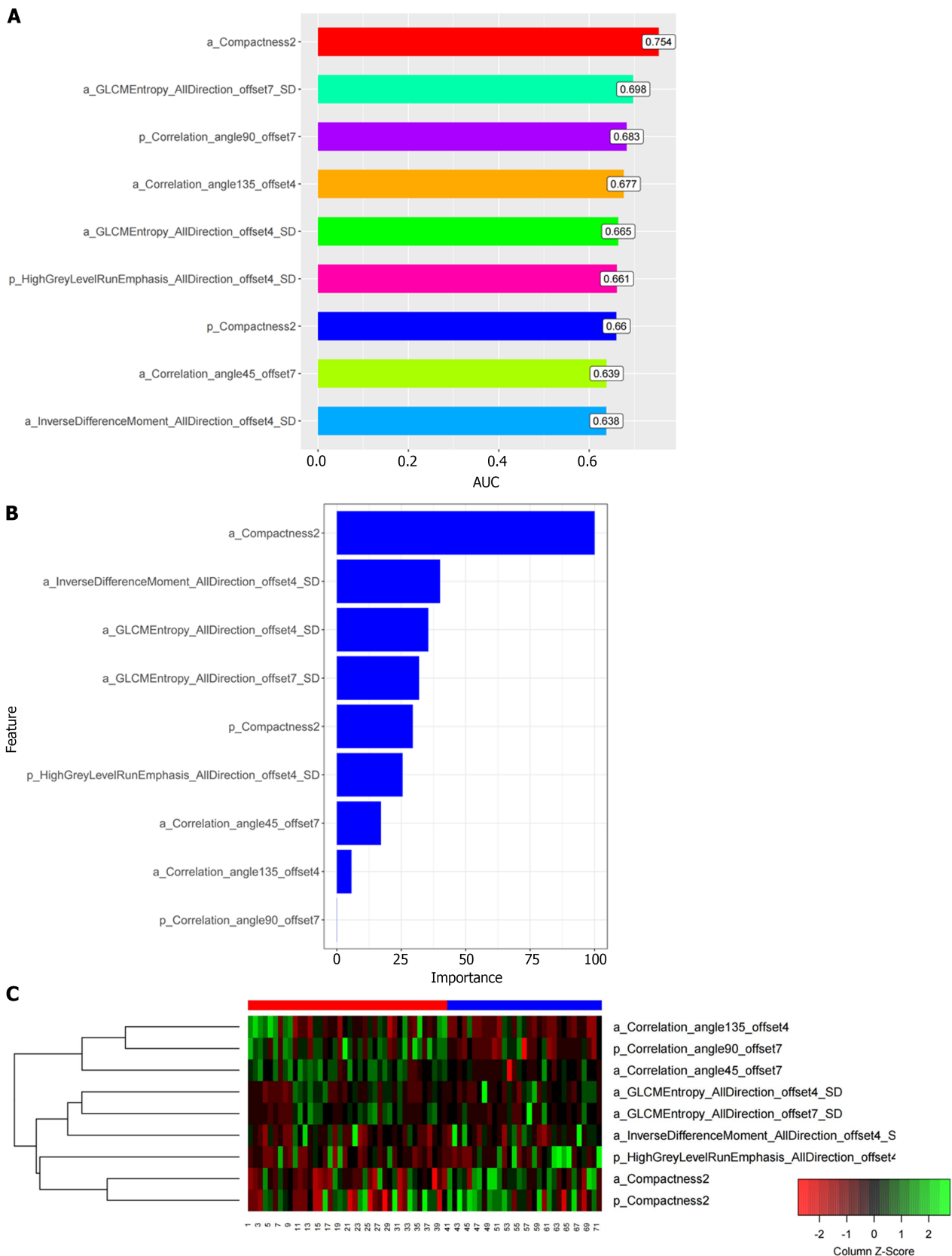


Figure 4 The area under receiver operating characteristic curve barplot, importance, and heatmap showing expression values of the selected features. The feature importance plot was provided by the random forest methods as soon as the model train procedure completed. The importance of the feature was computed from permuting out-of-bag data. A: The area under receiver operating characteristic curve barplot of the selected predictive radiomics features; B: The importance of the selected predictive radiomics features; C: The heatmap showing expression values of the selected radiomics features (rows) of 71 pancreatic ductal adenocarcinoma patients (columns). AUC: Area under the receiver operating characteristic curve.

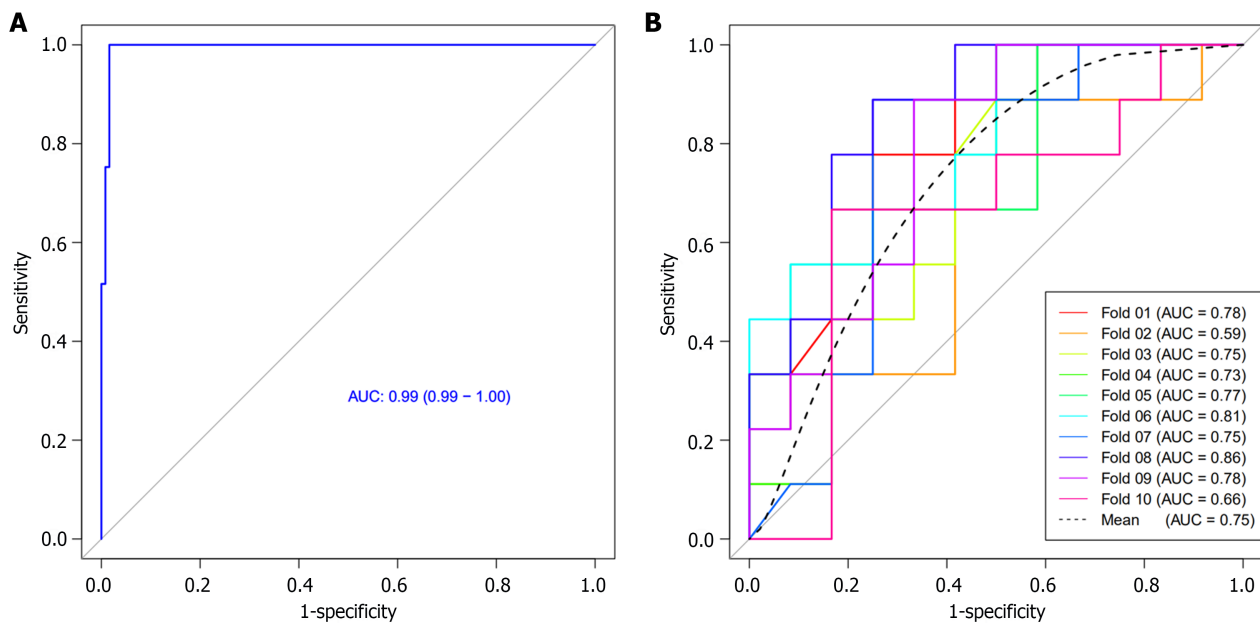


Figure 5 Receiver operating characteristic curve of the radiomics model and receiver operating characteristic curves of 10-times leave group out cross-validation analysis in differential diagnosis between early and late-stage pancreatic ductal adenocarcinoma. A: Receiver operating characteristic (ROC) curve of the radiomics model based on computed tomography images in the differentiation of early and late-stage pancreatic ductal adenocarcinoma (PDAC); B: ROC curves of 10-times leave group out cross-validation analysis for the differentiation of early and late stage PDAC, with a mean area under the curve of 0.75 by the average performance of the 10 newly built models, indicating good predictive ability of the radiomics model. AUC: Area under the receiver operating characteristic curve.

PDAC [24 (60%) *vs* 0 (0%), $P < 0.001$] since 24 patients with stage IV PDAC were included in late-stage PDAC group. Similarly, the sensitivity is low since stage III PDAC does not occur distant metastasis.

Recently, some researchers have investigated the potential value of CT texture analysis in predicting the overall survival of PDAC patients and evaluating the resectability of PDAC[23]. Our latest research study also investigated the potential value of CT texture analysis for prediction of histopathological grade of PDAC[24]. Fifty-six PDAC patients were divided into low-grade and high-grade; the CT texture analysis based on support vector machine achieved 78% sensitivity, 95% specificity, and 86% accuracy. In the present study, we developed and validated a radiomics model in differentiating early-stage PDAC from late-stage PDAC. A total of 792 radiomics features (396 from the late arterial phase and 396 from the portal venous phase) were extracted from the ROI for each case. Nine most important and predictive radiomics features were identified after feature selection using Mann-Whitney *U* test, univariate logistic regression analysis, and MRMR method. Among which, 6 features were extracted from the late arterial phase and the others from the portal venous phase. RF method was used to construct a radiomics model, which shows a high predictive ability with an AUC of 0.99; subsequently, 10-times LGOCV method was used to validate the robustness and reproducibility of the radiomics model, with a mean AUC of 0.75 by the average performance of the 10 newly built models, indicating good predictive ability of the radiomics model.

There were several limitations in this study. First, the weak point of this paper is that the methods are very difficult for clinicians, even radiologists, to understand[21]. Therefore, specialized knowledge is required to understand radiomics or radcores. However, current radiomics work was dominated by analysis of semantic, radiologist-defined features and carried qualitative real-world meaning. Radiomics is similar to a black box in that only a fraction of the features can be interpreted at present. Second, the enrolled number of patients was relatively small due to the strict inclusion criteria. Multicenter validated prospective studies would be necessary to validate these promising outcomes. Third, the retrospective nature of this study inherently introduces a selection bias. However, the fact is that most research regarding texture analysis or machine learning is retrospective in nature[24]. Forth, this study only investigates the potential value of radiomics in PDAC staging differential diagnosis; the role of other imaging techniques including MRI and postoperative radiotherapy/MR has not been discussed. This is mainly due to the fact that CT-based radiomics to predict the histological grade of PDAC is more conducive to generalization since it only uses CT which is fast, low cost, and widely available for processing without additional expenses. Additionally, the National Comprehensive Cancer Network guideline recommends serial CT with contrast for routine follow-up to determine therapeutic benefit.

CONCLUSION

In conclusion, we developed and validated a radiomics model in differentiating early-stage PDAC from late-stage PDAC. The radiomics model incorporating the most important and predictive features had a high discriminative ability.

ARTICLE HIGHLIGHTS

Research background

Pancreatic ductal adenocarcinoma (PDAC) remains the deadliest of the common cancers, with little change in patient survival in the past several decades. One of the biggest challenges of the management of PDAC that physicians often encounter is that the early detection in high-risk individuals and the early diagnosis of patients with suspected symptoms. Precise staging of PDAC is vital not only in making treatment decisions, but also in evaluating prognosis.

Research motivation

Radiomics, the generation of minable high throughput data through conversion of digital computed tomography (CT) or magnetic resonance imaging images, allows obtaining additional insight into pancreatic tissue heterogeneity. CT-based radiomics diagnostic approach could serve as a promising non-invasive method in differential diagnosis between early- and late-stage PDAC.

Research objectives

This study aimed to develop a radiomics-based diagnostic approach with a robust noninvasive diagnostic potential for identifying patients with early-stage PDAC.

Research methods

A total of 71 patients with pathologically proved PDAC based on surgical resection who underwent contrast-enhanced-CT within 30 d prior to surgery were included in the study. Radiomics features were extracted from the region of interest (ROI) for each patient using Analysis Kit software. The most important and predictive radiomics features were selected using Mann-Whitney *U* test, univariate logistic regression analysis, and minimum redundancy maximum relevance (MRMR) method. Random forest (RF) method was used to construct the radiomics model, and 10-times leave group out cross-validation (LGOCV) method was used to validate the robustness and reproducibility of the model.

Research results

A total of 792 radiomics features (396 from late arterial phase and 396 from portal venous phase) were extracted from the ROI for each patient. Nine most important and predictive features were selected using Mann-Whitney *U* test, univariate logistic regression analysis, and MRMR method. RF method was used to construct the radiomics model with the nine most predictive radiomics features, which showed a high discriminative ability with 97.7% accuracy, 97.6% sensitivity, 97.8% specificity, 98.4% positive predictive value, and 96.8% negative predictive value. The radiomics model was proved to be robust and reproducible using 10-times LGOCV method with an average area under the curve of 0.75 by the average performance of the 10 newly built models.

Research conclusions

This study demonstrated that CT-based radiomics diagnostic approach could be used to differentiate between early- and late-stage PDAC.

Research perspectives

This study developed a radiomics-based diagnostic approach with a robust noninvasive diagnostic potential for identifying patients with early-stage PDAC. Large-scale prospective cohort studies, preferably multi-center, to validate the potential value of the radiomics diagnostic approach in differentiating early from late stage PDAC are in order.

ACKNOWLEDGEMENTS

We thank all authors for their continuous and excellent support with patient data collection, imaging analysis, statistical analysis and valuable suggestions for the article.

FOOTNOTES

Co-first authors: Shuai Ren and Li-Chao Qian.

Co-corresponding authors: Ying Tian and Zhong-Qiu Wang.

Author contributions: Ren S and Qian LC contributed equally to this work; Ren S, Tian Y, and Wang ZQ designed the research study; Ren S, Qian LC, and Cao YY performed the research; Ren S, Qian LC, and Song LN analyzed the data; Ren S and Qian LC wrote the manuscript; Daniels MJ, Tian Y, and Wang ZQ revised the manuscript; and all authors read and approved the final manuscript. Tian Y and Wang ZQ contributed equally to this work as co-corresponding authors due to the fact that they contributed efforts of equal substance throughout the research process, such as facilitating communication with the journal, handling revisions, and addressing queries. Indeed, we believe that designating Tian Y and Wang ZQ as co-corresponding authors is fitting for our manuscript as it accurately reflects our team's collaborative spirit, equal contributions, and diversity.

Supported by the National Natural Science foundation of China, No. 82202135, 82371919, 82372017, and 82171925; China Postdoctoral Science Foundation, No. 2023M741808; Young Elite Scientists Sponsorship Program by Jiangsu Association for Science and Technology, No. JSTJ-2023-WJ027; Foundation of Excellent Young Doctor of Jiangsu Province Hospital of Chinese Medicine, No. 2023QB0112; Nanjing Postdoctoral Science Foundation, Natural Science Foundation of Nanjing University of Chinese Medicine, No. XZR2023036 and XZR2021050; and Medical Imaging Artificial Intelligence Special Research Fund Project, Nanjing Medical Association Radiology Branch, Project of National Clinical Research Base of Traditional Chinese Medicine in Jiangsu Province, China, No. JD2023SZ16.

Institutional review board statement: The study was reviewed and approved by the ethics committee of Affiliated Hospital of Nanjing University of Chinese Medicine (Approval No. 2017NL-137-05).

Informed consent statement: Informed consent statement was waived due to the retrospective nature of the study.

Conflict-of-interest statement: All the authors report no relevant conflicts of interest for this article.

Data sharing statement: Patient imaging data and histopathology reports contain sensitive patient information and cannot be released publicly due to the legal and ethical restrictions imposed by the institutional ethics committee (Affiliated Hospital of Nanjing University of Chinese Medicine). Data is available upon reasonable request from the following e-mail address: zhongqiuwang@njucm.edu.cn.

Open-Access: This article is an open-access article that was selected by an in-house editor and fully peer-reviewed by external reviewers. It is distributed in accordance with the Creative Commons Attribution NonCommercial (CC BY-NC 4.0) license, which permits others to distribute, remix, adapt, build upon this work non-commercially, and license their derivative works on different terms, provided the original work is properly cited and the use is non-commercial. See: <https://creativecommons.org/licenses/by-nc/4.0/>

Country/Territory of origin: China

ORCID number: Shuai Ren 0000-0003-4902-6298; Li-Chao Qian 0009-0006-3071-3011; Ying-Ying Cao 0000-0001-9067-6319; Marcus J Daniels 0000-0003-1209-1918; Li-Na Song 0000-0001-6547-335X; Ying Tian 0000-0002-1525-0614; Zhong-Qiu Wang 0000-0001-6681-7345.

S-Editor: Wang JJ

L-Editor: A

P-Editor: Cai YX

REFERENCES

- 1 Siegel RL, Miller KD, Wagle NS, Jemal A. Cancer statistics, 2023. *CA Cancer J Clin* 2023; **73**: 17-48 [PMID: 36633525 DOI: 10.3322/caac.21763]
- 2 Miller FH, Lopes Vendrami C, Hammond NA, Mittal PK, Nikolaidis P, Jawahar A. Pancreatic Cancer and Its Mimics. *Radiographics* 2023; **43**: e230054 [PMID: 37824413 DOI: 10.1148/rg.230054]
- 3 Guler GD, Ning Y, Ku CJ, Phillips T, McCarthy E, Ellison CK, Bergamaschi A, Collin F, Lloyd P, Scott A, Antoine M, Wang W, Chau K, Ashworth A, Quake SR, Levy S. Detection of early stage pancreatic cancer using 5-hydroxymethylcytosine signatures in circulating cell free DNA. *Nat Commun* 2020; **11**: 5270 [PMID: 33077732 DOI: 10.1038/s41467-020-18965-w]
- 4 Nagai M, Nakamura K, Terai T, Kohara Y, Yasuda S, Matsuo Y, Doi S, Sakata T, Sho M. Significance of multiple tumor markers measurements in conversion surgery for unresectable locally advanced pancreatic cancer. *Pancreatol* 2023; **23**: 721-728 [PMID: 37328387 DOI: 10.1016/j.pan.2023.06.001]
- 5 Kim SS, Lee S, Lee HS, Bang S, Han K, Park MS. Retrospective Evaluation of Treatment Response in Patients with Nonmetastatic Pancreatic Cancer Using CT and CA 19-9. *Radiology* 2022; **303**: 548-556 [PMID: 35258374 DOI: 10.1148/radiol.212236]
- 6 Coppola A, La Vaccara V, Fiore M, Farolfi T, Ramella S, Angeletti S, Coppola R, Caputo D. CA19.9 Serum Level Predicts Lymph-Nodes Status in Resectable Pancreatic Ductal Adenocarcinoma: A Retrospective Single-Center Analysis. *Front Oncol* 2021; **11**: 690580 [PMID: 34123859 DOI: 10.3389/fonc.2021.690580]
- 7 Huang B, Huang H, Zhang S, Zhang D, Shi Q, Liu J, Guo J. Artificial intelligence in pancreatic cancer. *Theranostics* 2022; **12**: 6931-6954 [PMID: 36276650 DOI: 10.7150/thno.77949]
- 8 Zhang L, Sanagapalli S, Stoitia A. Challenges in diagnosis of pancreatic cancer. *World J Gastroenterol* 2018; **24**: 2047-2060 [PMID: 29785074 DOI: 10.3748/wjg.v24.i19.2047]
- 9 Cheng H, Luo G, Jin K, Xiao Z, Qian Y, Gong Y, Yu X, Liu C. Predictive Values of Preoperative Markers for Resectable Pancreatic Body and Tail Cancer Determined by MDCT to Detect Occult Metastases. *World J Surg* 2021; **45**: 2185-2190 [PMID: 33774691 DOI: 10.1007/s00268-021-06047-x]
- 10 Ahmed SA, Atta H, Hassan RA. The utility of Multi-Detector Computed Tomography criteria after neoadjuvant therapy in Borderline Resectable Pancreatic cancer: Prospective, bi-institutional study. *Eur J Radiol* 2021; **139**: 109685 [PMID: 33819805 DOI: 10.1016/j.ejrad.2021.109685]
- 11 Kulkarni NM, Soloff EV, Tolat PP, Sangster GP, Fleming JB, Brook OR, Wang ZJ, Hecht EM, Zins M, Bhosale PR, Arif-Tiwari H, Mannelli L, Kambadakone AR, Tamm EP. White paper on pancreatic ductal adenocarcinoma from society of abdominal radiology's disease-focused panel for pancreatic ductal adenocarcinoma: Part I, AJCC staging system, NCCN guidelines, and borderline resectable disease. *Abdom Radiol (NY)* 2020; **45**: 716-728 [PMID: 31748823 DOI: 10.1007/s00261-019-02289-5]
- 12 Kulkarni NM, Mannelli L, Zins M, Bhosale PR, Arif-Tiwari H, Brook OR, Hecht EM, Kastrinos F, Wang ZJ, Soloff EV, Tolat PP, Sangster G, Fleming J, Tamm EP, Kambadakone AR. White paper on pancreatic ductal adenocarcinoma from society of abdominal radiology's disease-

- focused panel for pancreatic ductal adenocarcinoma: Part II, update on imaging techniques and screening of pancreatic cancer in high-risk individuals. *Abdom Radiol (NY)* 2020; **45**: 729-742 [PMID: [31768594](#) DOI: [10.1007/s00261-019-02290-y](#)]
- 13 **Berbis MÁ**, Godino FP, Rodríguez-Comas J, Nava E, García-Figueiras R, Baleato-González S, Luna A. Radiomics in CT and MR imaging of the liver and pancreas: tools with potential for clinical application. *Abdom Radiol (NY)* 2024; **49**: 322-340 [PMID: [37889265](#) DOI: [10.1007/s00261-023-04071-0](#)]
 - 14 **Xiao G**, Rong WC, Hu YC, Shi ZQ, Yang Y, Ren JL, Cui GB. MRI Radiomics Analysis for Predicting the Pathologic Classification and TNM Staging of Thymic Epithelial Tumors: A Pilot Study. *AJR Am J Roentgenol* 2020; **214**: 328-340 [PMID: [31799873](#) DOI: [10.2214/AJR.19.21696](#)]
 - 15 **Tabari A**, Chan SM, Omar OMF, Iqbal SI, Gee MS, Daye D. Role of Machine Learning in Precision Oncology: Applications in Gastrointestinal Cancers. *Cancers (Basel)* 2022; **15** [PMID: [36612061](#) DOI: [10.3390/cancers15010063](#)]
 - 16 **Xu C**, Jun E, Okugawa Y, Toiyama Y, Borazanci E, Bolton J, Taketomi A, Kim SC, Shang D, Von Hoff D, Zhang G, Goel A. A Circulating Panel of circRNA Biomarkers for the Noninvasive and Early Detection of Pancreatic Ductal Adenocarcinoma. *Gastroenterology* 2024; **166**: 178-190.e16 [PMID: [37839499](#) DOI: [10.1053/j.gastro.2023.09.050](#)]
 - 17 **Ren S**, Qian L, Daniels MJ, Duan S, Chen R, Wang Z. Evaluation of contrast-enhanced computed tomography for the differential diagnosis of hypovascular pancreatic neuroendocrine tumors from chronic mass-forming pancreatitis. *Eur J Radiol* 2020; **133**: 109360 [PMID: [33126171](#) DOI: [10.1016/j.ejrad.2020.109360](#)]
 - 18 **Ren S**, Chen X, Wang J, Zhao R, Song L, Li H, Wang Z. Differentiation of duodenal gastrointestinal stromal tumors from hypervascular pancreatic neuroendocrine tumors in the pancreatic head using contrast-enhanced computed tomography. *Abdom Radiol (NY)* 2019; **44**: 867-876 [PMID: [30293109](#) DOI: [10.1007/s00261-018-1803-x](#)]
 - 19 **Tempero MA**, Malafa MP, Chiorean EG, Czito B, Scaife C, Narang AK, Fountzilaz C, Wolpin BM, Al-Hawary M, Asbun H, Behrman SW, Benson AB, Binder E, Cardin DB, Cha C, Chung V, Dillhoff M, Dotan E, Ferrone CR, Fisher G, Hardacre J, Hawkins WG, Ko AH, LoConte N, Lowy AM, Moravek C, Nakakura EK, O'Reilly EM, Obando J, Reddy S, Thayer S, Wolff RA, Burns JL, Zuccarino-Catania G. Pancreatic Adenocarcinoma, Version 1.2019. *J Natl Compr Canc Netw* 2019; **17**: 202-210 [PMID: [30865919](#) DOI: [10.6004/jnccn.2019.0014](#)]
 - 20 **Ren S**, Zhang J, Chen J, Cui W, Zhao R, Qiu W, Duan S, Chen R, Chen X, Wang Z. Evaluation of Texture Analysis for the Differential Diagnosis of Mass-Forming Pancreatitis From Pancreatic Ductal Adenocarcinoma on Contrast-Enhanced CT Images. *Front Oncol* 2019; **9**: 1171 [PMID: [31750254](#) DOI: [10.3389/fonc.2019.01171](#)]
 - 21 **Ren S**, Zhao R, Cui W, Qiu W, Guo K, Cao Y, Duan S, Wang Z, Chen R. Computed Tomography-Based Radiomics Signature for the Preoperative Differentiation of Pancreatic Adenosquamous Carcinoma From Pancreatic Ductal Adenocarcinoma. *Front Oncol* 2020; **10**: 1618 [PMID: [32984030](#) DOI: [10.3389/fonc.2020.01618](#)]
 - 22 **Ma C**, Yang P, Li J, Bian Y, Wang L, Lu J. Pancreatic adenocarcinoma: variability in measurements of tumor size among computed tomography, magnetic resonance imaging, and pathologic specimens. *Abdom Radiol (NY)* 2020; **45**: 782-788 [PMID: [31292672](#) DOI: [10.1007/s00261-019-02125-w](#)]
 - 23 **Cassinotto C**, Chong J, Zogopoulos G, Reinhold C, Chiche L, Lafourcade JP, Cuggia A, Terrebonne E, Dohan A, Gallix B. Resectable pancreatic adenocarcinoma: Role of CT quantitative imaging biomarkers for predicting pathology and patient outcomes. *Eur J Radiol* 2017; **90**: 152-158 [PMID: [28583627](#) DOI: [10.1016/j.ejrad.2017.02.033](#)]
 - 24 **Qiu W**, Duan N, Chen X, Ren S, Zhang Y, Wang Z, Chen R. Pancreatic Ductal Adenocarcinoma: Machine Learning-Based Quantitative Computed Tomography Texture Analysis For Prediction Of Histopathological Grade. *Cancer Manag Res* 2019; **11**: 9253-9264 [PMID: [31802945](#) DOI: [10.2147/CMAR.S218414](#)]



Published by **Baishideng Publishing Group Inc**
7041 Koll Center Parkway, Suite 160, Pleasanton, CA 94566, USA

Telephone: +1-925-3991568

E-mail: office@baishideng.com

Help Desk: <https://www.f6publishing.com/helpdesk>

<https://www.wjgnet.com>

